

Seismicity and GPS constraints on crustal deformation in the southern part of the Korean Peninsula

Shuanggen Jin* *Space Geodesy Division, Korea Astronomy and Space Science Institute, Daejeon 305-348, South Korea*
Shanghai Astronomical Observatory, Chinese Academy of Sciences, Shanghai 200030, China
Z.C. Li *Geodesy Department, National Geomatics Center of China, Beijing 100044, China*
Pil-Ho Park *Space Geodesy Division, Korea Astronomy and Space Science Institute, Daejeon 305-348, South Korea*

ABSTRACT: Three years of continuous observations at 45 GPS sites in South Korea show horizontal deformation velocities are less than 3 mm/yr with respect to the stable South Korea block. These velocities and the associated horizontal strain rate reveal that South Korea is dominated by both ENE-WSW compression and NNW-SSE extension. Compared to the seismic strain rate in South Korea derived from recently recorded earthquake data ($M_w > 4.0$, 1936-2004), the principal horizontal axes of both strain rate tensors are nearly consistent, indicating that the seismicity can be used to improve GPS-derived deformation style and orientation. In addition, it also reflects that the occurrence of shallow earthquakes in South Korea is closely related with the horizontal strain.

Key words: Crustal deformation, GPS, Seismicity, Strain rate, Korean Peninsula

1. INTRODUCTION

Although the Korean Peninsula is located in the East Asian active edge between the Eurasian and Pacific plates (Molnar and Tapponnier, 1975; Kato et al., 1998; Kogan et al., 2000), with respect to highly seismic surrounding zones (SW Japan, North China and Sakhalin) (Kim et al. 2004), the earthquake activity in the Korean Peninsula is relatively low and shallow with magnitudes ranging from 2.0 to 5.5 on Richter scale and depths ranging from 10 to 20 km (Jun, 1993). However, historical records show that several large earthquakes in Korea have resulted in human casualties and serious property damages, such as building breaking down, landslide, etc. Accurate measurement of crustal deformation in the Korean Peninsula will contribute to our understanding of the tectonic features, to decode the physical processes of tectonic activities (such as earthquakes) and to evaluate or mitigate earthquake risk. The existing permanent Korean GPS Network (KGN) provides an important data set to investigate present-day crustal deformation in the southern part of the Korean Peninsula and a fundamental tool in seismic risk evaluation and earthquake prediction research.

In addition, historically recorded earthquake data can fur-

ther provide some deformation features of tectonic activities. Comparison of the seismic and geodetic deformation is important both for understanding tectonic deformation and for earthquake hazard assessment (Masson et al. 2005). Therefore, combined with the earthquake data, the deformation parameters (style, direction and rate) are well suited to accurately define the deformation pattern and to distinguish the seismic from aseismic deformation and even to evaluate earthquake risk. In this paper, we aim to investigate crustal deformation using the existing permanent Korean GPS Network (KGN) and recently recorded earthquake data ($M_w > 4.0$, 1936-2004), and to evaluate the relationship between deformation recorded with GPS and seismicity in South Korea.

2. GPS DERIVED CRUSTAL DEFORMATION

2.1. GPS Velocity Field

The permanent Korean GPS Network (KGN) has been established since 2000, and daily observation data are transferred to the data center. Most raw data can be downloaded soon from the global data center (GDC) in the Korea Astronomy and Space Science Institute (KASI) (<http://gdc.kasi.re.kr>). The KGN provides real observation data to monitor present-day crustal deformation in South Korea. We analyzed all available good data for the period from March 2000 to August 2003 using scientific GAMIT software (King and Bock, 1999) with IGS precise orbits and IGS Earth Rotation Parameters. All loosely constrained solutions for each day are then combined using the GLOBK, and the reference frame is applied to the solution by performing a seven-parameter transformation to align it to ITRF2000 with global 54 core stations (Altamimi et al. 2002). The site velocities are estimated by least square linear fitting to time variation of the daily coordinates for each station. The 1-sigma quality of each station is 0.7-1.1 mm/yr for NS component and 0.3-1.9 mm/yr for EW-component as well as 1.1-2.6 mm/yr for vertical component. The GPS stations and velocity field are shown in Table 1 and Figure 1.

*Corresponding author: sgjin@kasi.re.kr

Table 1. GPS stations and deformation velocity field respective to the South Korea block (Unit: mm/yr)

Sites	Lon	Lat	Vn	Ve	Sig_vn	Sig_Ve	Observed time
DAEJ	127.37	36.40	-0.50	-0.04	0.98	1.04	2000/03-2003/08
HONC	128.19	37.71	-2.13	-1.57	1.02	1.30	2000/03-2003/08
DOND	127.06	37.90	-1.21	-0.74	1.00	1.21	2000/03-2003/08
WNJU	127.95	37.34	-0.31	-1.58	0.96	1.04	2000/03-2003/08
SNJU	128.14	36.38	0.22	-1.05	1.07	1.39	2000/11-2003/08
INCH	126.69	37.42	-2.59	-0.51	0.98	1.01	2000/03-2003/08
CHYG	126.80	36.46	-1.22	0.48	0.97	1.02	2000/03-2003/08
CNJU	127.46	36.63	-2.38	1.02	1.00	1.09	2000/11-2003/08
MUJU	127.66	36.00	-1.08	-0.80	0.98	1.04	2000/03-2003/08
GSAN	127.79	36.82	-0.97	-0.42	0.97	1.03	2000/03-2003/08
SEOS	126.49	36.78	-0.73	0.57	0.99	1.06	2000/08-2003/08
KIMC	128.14	36.14	-0.21	0.75	1.03	1.29	2000/10-2003/08
NONS	127.10	36.19	-2.49	-0.29	0.97	1.11	2000/03-2003/08
CHLW	127.42	38.16	-2.37	-1.13	1.01	1.05	2000/03-2003/08
KANR	128.87	37.77	0.63	-0.43	0.96	1.00	2001/07-2003/08
CHCN	127.71	37.87	-1.35	-0.50	1.01	1.35	2000/03-2003/08
PAJU	126.74	37.75	0.23	-1.84	1.00	1.25	2000/03-2003/08
SOUL	127.08	37.63	-1.71	-0.96	0.98	1.10	2000/12-2003/08
SKMA	126.92	37.49	-1.69	-0.27	1.02	1.25	2000/03-2003/08
YANP	127.51	37.45	-1.15	-1.41	1.02	1.30	2000/03-2003/08
SUWN	127.05	37.28	-1.78	0.55	1.04	1.39	2000/03-2003/08
SKCH	128.56	38.25	-0.44	-0.91	0.97	1.03	2000/03-2003/08
YOWL	128.46	37.18	-0.23	-0.63	0.95	0.98	2000/03-2003/08
WULJ	129.41	36.99	0.64	-0.64	0.97	1.00	2000/03-2003/08
SBAO	128.46	36.93	0.69	-2.69	0.96	1.02	2000/08-2003/08
YECH	128.45	36.65	0.40	-0.54	0.95	0.98	2000/10-2003/08
BHAO	128.98	36.16	-0.22	0.17	0.99	1.05	2000/03-2003/08
KUNW	128.57	36.23	1.13	0.68	0.95	1.00	2000/03-2003/08
TEGN	128.80	35.91	-0.08	0.26	0.98	1.10	2000/03-2003/08
WOLS	129.42	35.51	0.73	-0.92	1.03	1.22	2000/03-2003/08
MLYN	128.74	35.49	-0.61	-0.28	1.01	1.18	2000/03-2003/08
PUSN	129.07	35.23	-2.30	-1.05	0.99	1.13	2000/08-2003/08
JINJ	128.05	35.17	-0.48	-0.93	0.99	1.13	2000/03-2003/08
GOCH	127.94	35.67	0.40	-1.58	0.99	1.12	2000/03-2003/08
NAMW	127.40	35.42	-0.49	0.35	0.98	1.09	2000/03-2003/08
KWNJ	126.91	35.18	-1.10	0.10	0.98	1.12	2000/11-2003/08
SONC	127.49	34.96	0.09	-0.85	0.90	0.91	2000/08-2003/08
MKPO	126.38	34.82	-1.91	0.08	0.90	0.92	2000/07-2003/08
JEJU	126.46	33.29	0.82	0.33	0.95	1.22	2000/04-2003/08
CHNG	128.48	35.53	1.45	0.63	1.00	1.26	2001/03-2003/08
JUNJ	127.14	35.84	0.09	0.76	0.99	1.15	2000/03-2003/08
JUNG	126.97	35.62	-2.18	-0.63	0.96	1.04	2000/03-2003/08
INJE	128.17	38.07	-0.84	-0.81	0.98	1.06	2000/03-2003/08
SNPA	126.62	33.38	0.93	0.28	1.10	1.41	2000/03-2003/08
CHJU	126.53	33.51	-1.24	0.43	0.93	1.24	2000/07-2003/08

2.2. Euler vector for the South Korea block

In order to analyze the intraplate deformation in South Korea, firstly we eliminate the rigid rotation motion. The NNR-NUVEL-1A model was determined from the geolog-

ical and geophysical data in the past 3 million years (DeMets et al., 1990) and may not well represent the present-day background field. Furthermore, the Euler vector for the Eurasian plate cannot well describe the overall motions of East Asia (including South Korea). Therefore, it is desirable to

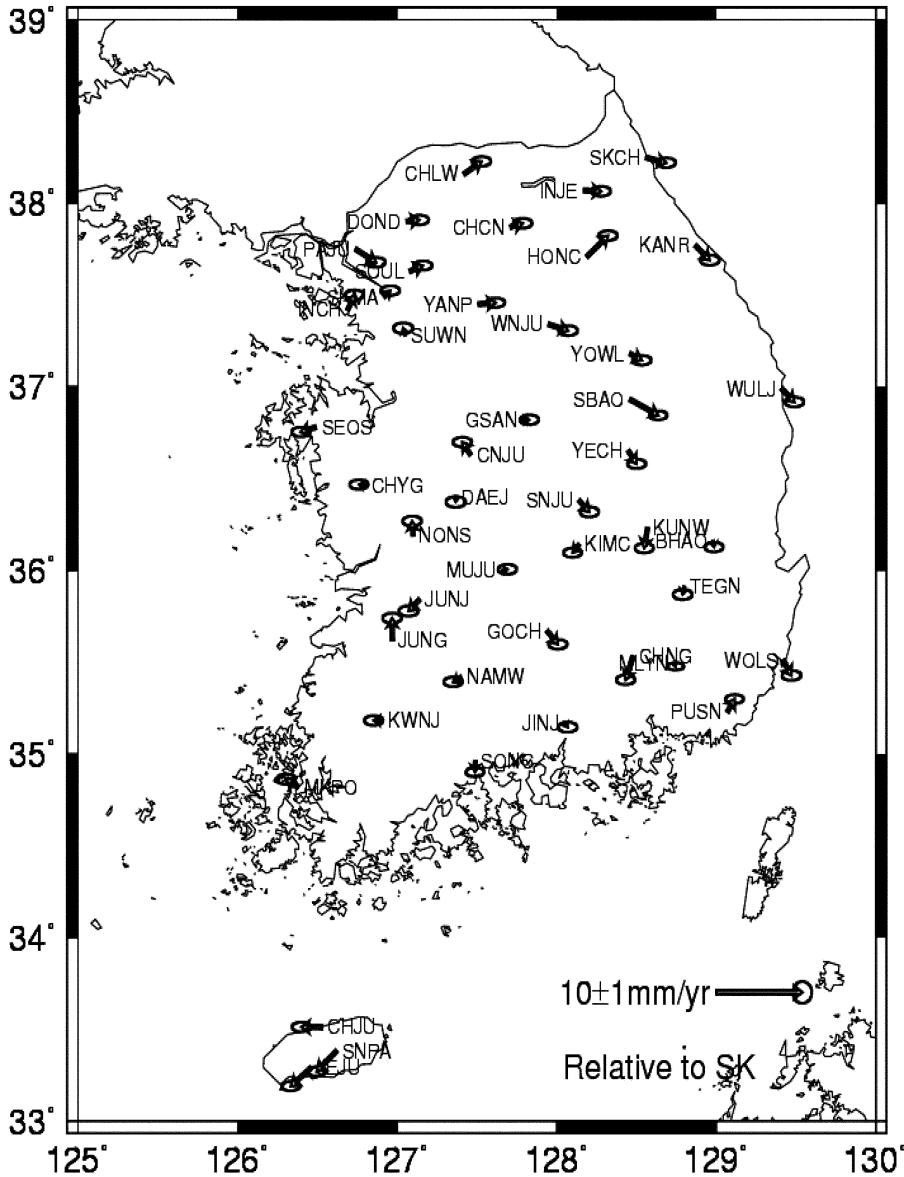


Fig. 1. GPS horizontal deformation velocities and their 95% confidence ellipses in the South Korea block-fixed reference frame. GPS stations are indicated by capital letters and the arrows show the GPS deformation velocities.

establish a suitable block motion model of South Korea using current space geodetic data. According to the theory of Euler plate motion, the Euler rotation vector can be determined (DeMets et al., 1990), as

$$\vec{v}_i = \vec{\Omega} \times \vec{r}_i \quad (1)$$

where \vec{v}_i and \vec{r}_i are the velocity and position vectors of station i , respectively, and $\vec{\Omega}$ is the Euler rotation vector. Because the plate motion mainly focuses on the horizontal direction, and moreover, the precision of vertical station velocity is low, only horizontal velocities are used to calculate the Euler rotation vector of plate motion. Thus the Eq. (1) can be written as the following matrix equation:

$$\begin{bmatrix} v_n \\ v_e \end{bmatrix} = \begin{bmatrix} r \sin \lambda & -r \cos \lambda & 0 \\ -r \sin \phi \cos \lambda & -r \sin \phi \sin \lambda & r \cos \phi \end{bmatrix} \begin{bmatrix} \Omega_x \\ \Omega_y \\ \Omega_z \end{bmatrix} \quad (2)$$

where v_n and v_e are the north velocity and east velocity, respectively, λ and ϕ are the longitude and latitude, respectively, and r is the radius of the Earth. If there are more than two stations in one plate or block, the Euler rotation parameters can be estimated through a weighted least squares algorithm in Eq (2),

$$\Omega = \sqrt{\Omega_x^2 + \Omega_y^2 + \Omega_z^2}$$

$$\alpha = \text{tg}^{-1} \frac{\Omega_y}{\Omega_x}$$

$$\beta = tg^{-1} \frac{\Omega_z}{\sqrt{\Omega_x^2 + \Omega_y^2}} \quad (3)$$

where Ω is the Euler rotation rate, α and β are the Euler rotation longitude and latitude, respectively. Here we used the 10 GPS velocity field of the KGN GPS network to fit the Euler's vector of South Korea block motion. Our fitting estimate of the angular velocity vector has a rotation rate of $0.329 \pm 0.004^\circ/\text{Ma}$ at the pole of $-130.77 \pm 1.1^\circ\text{E}$ and $64.18 \pm 0.7^\circ\text{N}$. The Euler vector that describes the present-day motion of South Korea can be regarded as a better motion model than the geological model NNR-NUVEL-1A averaged in the past 3 million years (DeMets et al., 1990; Jin and Zhu, 2004).

2.3. Deformation Rates

The intra-plate deformation rates in South Korea are obtained by eliminating the entire rigid motion of the South Korea block based on the Euler vector. Figure 1 shows the GPS horizontal deformation residual velocities and their 95% confidence ellipses in the South Korea block-fixed reference frame. The deformation rates are less than 3 mm/yr and the average deformation rate is about 1.5 mm/yr, which reflects that South Korea is almost rigid and stable. The overall deformation motions of all sites in South Korea are rotating clockwise, and extending in North-South direction and slightly shortening in West-East direction. In addition, the three stations (JEJU, CHJU and SNPA) in Jeju Island are obviously moving westward, indicating that the Jeju Island is slightly subject to west extrusion of the southwest Japanese Island Arc.

In order to further investigate the entire deformation pattern of South Korea, the crustal strain rate in South Korea is derived from GPS horizontal deformation velocities by (Calais et al., 2000):

$$\begin{aligned} v_{ei} &= \frac{\partial v_{ei}}{\partial x_{ei}} x_{ei} + \frac{\partial v_{ei}}{\partial x_{ni}} x_{ni} \\ v_{ni} &= \frac{\partial v_{ni}}{\partial x_{ei}} x_{ei} + \frac{\partial v_{ni}}{\partial x_{ni}} x_{ni} \end{aligned} \quad (4)$$

where v_{ei} and v_{ni} are the east and north component velocity at the site i located at (x_{ei}, x_{ni}) . Strain components $\dot{\epsilon}_{ee}$, $\dot{\epsilon}_{nn}$ and $\dot{\epsilon}_{en}$ are expressed as $\frac{\partial v_e}{\partial x_e}$, $\frac{\partial v_n}{\partial x_n}$ and $\frac{1}{2} \left(\frac{\partial v_e}{\partial x_n} + \frac{\partial v_n}{\partial x_e} \right)$, respectively. The maximum principal strain $\dot{\epsilon}_1$ and the minimum principal strain $\dot{\epsilon}_2$ are given by:

$$\dot{\epsilon}_1, \dot{\epsilon}_2 = \frac{1}{2} (\dot{\epsilon}_{ee} + \dot{\epsilon}_{nn}) \pm \sqrt{\frac{1}{4} (\dot{\epsilon}_{ee} - \dot{\epsilon}_{nn})^2 + (\dot{\epsilon}_{en})^2} \quad (5)$$

with directions θ and $\theta + (\pi/2)$, with θ given by:

$$\tan(2\theta) = \frac{2\dot{\epsilon}_{en}}{\dot{\epsilon}_{ee} - \dot{\epsilon}_{nn}} \quad (6)$$

Thus, using the GPS velocity field in Table 1, the principal strain rate of South Korea can be obtained through the weighted least squares algorithm, showing in Table 4 and Figure 3. The principal axis of extension is NNW-SSE and the principal axis of compression is WSW-ENE, which shows that South Korea is under both compression in WSW-ENE and extension in NNW-SSE. This also coincides with the crustal deformation trend revealed by GPS deformation velocity field with respect to the South Korea block (Fig. 1).

3. SEISMICITY-DERIVED CRUSTAL DEFORMATION

3.1. Seismic activities in Korea

In the past 2000 years, there are many small and low earthquakes in and around the southern part of the Korean peninsula, ranging from 2.0 to 5.5 on Richter scale. We collected available data of earthquakes recorded during the period from 1936-2004 with $M_w > 4.0$ in and around South Korea and the epicenters of earthquakes are shown in Table 2 and Figure 2. The earthquake data might contribute to reveal the tectonic features and deformation style and pattern in the southern part of the Korean peninsula. Other small earthquakes with $M_w > 4.0$ are not considered because they are assumed to have a negligible effect on tectonic motions.

3.2. Seismic Strain Rate Tensor

The relationship between the seismic strain rate tensor and seismic moment tensor was described by Kostrov (1974). If the deformation that occurs within a volume V containing active faults is seismic, the average seismic strain rate $\dot{\epsilon}_{ij}$ during a time t is as following (Kostrov, 1974):

$$\dot{\epsilon}_{ij} = \frac{1}{2\mu t V} \sum_{k=1}^N M_{ij}^k = \frac{1}{2\mu t A H_s} \sum_{k=1}^N M_{ij}^k \quad (7)$$

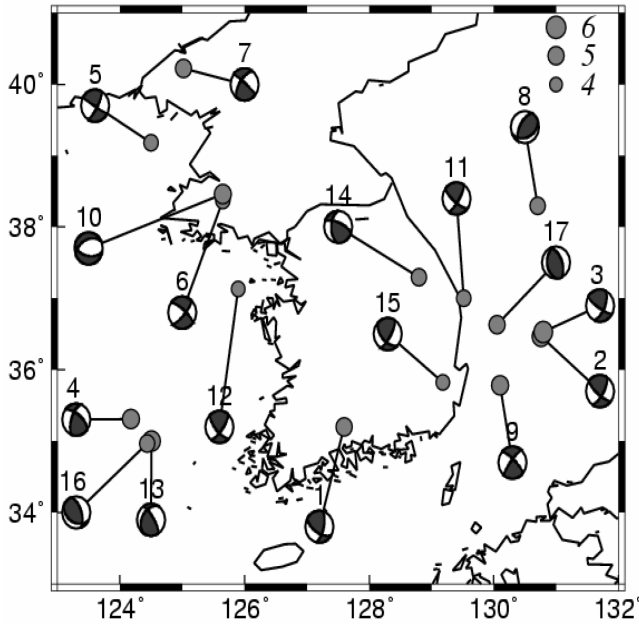
where μ is the shear modulus of rigidity, A is the study seismic area, H_s is the seismogenic depth, and M_{ij}^k is the components of the moment tensor M^k of earthquakes k . M^k is defined from the scalar moment M_0^k and the unit vector normal to the fault plane and the unit of vector in the direction of slip with the well-known expression (e.g. Jost and Herrmann, 1989):

$$M_{ij} = M_0(u_i n_j + u_j n_i) \quad (8)$$

where u and n , the normal and slip unit vectors, are a func-

Table 2. Source mechanism of earthquakes with $M_w > 4.0$ in and around South Korea

No.	Lon (°)	Lat (°)	strike (°)	dip (°)	slip (°)	Rake (°)	Magnitude	time yy/mm/dd	moment 10^{18} Nm
1	127.60	35.20	14.0	64.0	121.0	60.0	5.1	1936.07.04	0.056
2	130.76	36.47	32.0	69.0	129.0	72.0	5.7	1963.09.06	0.447
3	130.79	36.53	25.0	61.0	122.0	79.0	5.8	1963.09.07	0.631
4	124.18	35.31	199.5	61.8	306.8	61.0	5.4	1976.10.06	0.158
5	124.50	39.18	30.0	75.0	120.5	84.0	4.6	1978.08.29	0.010
6	125.65	38.37	43.0	75.0	308.5	75.0	4.5	1978.11.23	0.007
7	125.02	40.22	215.7	62.3	309.1	83.6	5.1	1980.01.07	0.056
8	130.70	38.30	210.0	60.0	66.0	35.5	4.9	1980.09.20	0.028
9	130.10	35.78	312.0	75.0	219.0	79.0	5.2	1981.04.15	0.079
10	125.65	38.46	245.2	43.8	100.6	52.0	5.3	1982.02.14	0.112
11	129.52	37.00	33.0	75.0	128.2	70.0	4.6	1982.02.28	0.010
12	125.90	37.13	37.5	70.0	137.0	65.0	4.2	1982.08.28	0.003
13	124.51	35.00	215.2	37.0	327.4	74.1	5.5	1994.07.25	0.224
14	128.80	37.30	181.0	50.0	292.0	65.0	4.8	1996.12.13	0.020
15	129.18	35.82	135.0	52.0	31.0	50.0	4.3	1997.06.26	0.004
16	124.44	34.97	340.0	60.0	200.0	30.5	4.9	2003.03.23	0.028
17	130.05	36.63	337.0	56.0	178.0	36.0	5.1	2004.05.29	0.056

**Fig. 2.** Epicentral distribution (solid circles) of major 17 events (with $M_w \geq 4.0$) in and around the southern part of the Korean peninsula from 1936 - 2004. Solid and open quadrants correspond to compression and dilatation.

tion of the strike, dip, and rake of the focal mechanism, and M_0 , the scalar seismic moment tensor (in Nm), may be calculated from the surface wave magnitude M_s by (Ekstrom and Dziewonski, 1988)

$$\log M_0 = 1.5M_s + 9.14 \quad (9)$$

In the usual right-handed coordinate systems (e: east, n:

Table 3. Seismic moment tensor and strain rates in South Korea

	Seismic moment tensor ($\times 10^{18}$ Nm/yr)	Seismic strain rate ($\times 10^{-9}$ /yr)
M_{ee}	-0.679	$\dot{\epsilon}_{ee}$ -0.028
M_{en}	0.745	$\dot{\epsilon}_{en}$ 0.031
M_{eu}	0.229	$\dot{\epsilon}_{eu}$ 0.009
M_{nn}	-0.759	$\dot{\epsilon}_{nn}$ -0.030
M_{nu}	-0.567	$\dot{\epsilon}_{nu}$ -0.023
M_{uu}	1.437	$\dot{\epsilon}_{uu}$ 0.059

north and u: vertical), the seismic moment tensor M_{ij}^k can be obtained by (Aki and Richards, 1980):

$$M_{nn} = -M_0(\cos\alpha \sin\gamma \sin 2\beta + \sin\alpha \sin 2\gamma \sin^2\beta)$$

$$M_{ne} = M_0\left(\cos\alpha \sin\gamma \sin 2\beta + \frac{1}{2}\sin\alpha \sin 2\gamma \sin 2\beta\right)$$

$$M_{nu} = -M_0(\cos\alpha \cos\gamma \cos\beta + \sin\alpha \cos 2\gamma \sin\beta)$$

$$M_{ee} = M_0(\cos\alpha \sin\gamma \sin 2\beta - \sin\alpha \cos 2\gamma \cos^2\beta)$$

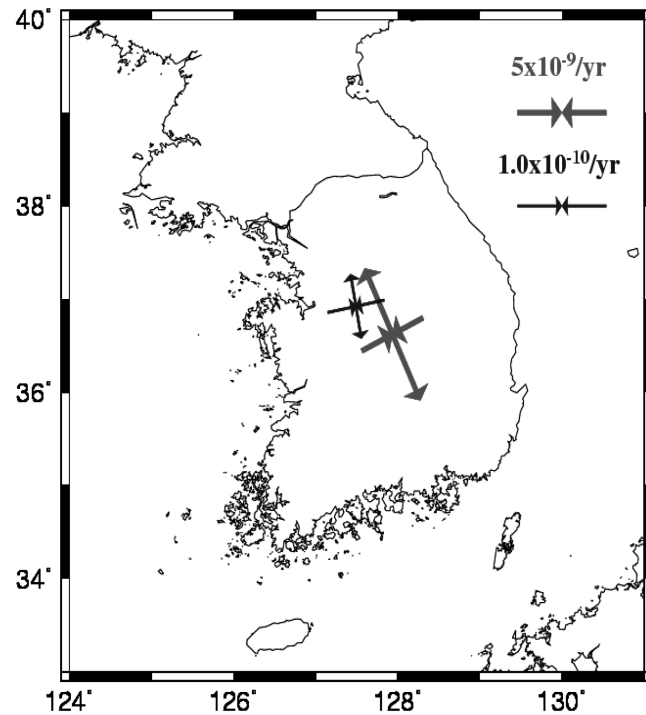
$$M_{eu} = -M_0(\cos\alpha \cos\gamma \cos\beta - \sin\alpha \cos 2\gamma \cos\beta)$$

$$M_{uu} = M_0(\sin\alpha \sin 2\beta) \quad (10)$$

Where α , β , and γ are the direction of slip, strike and dip, respectively. Here the average seismical depth is 15 km, the study seismic area is South Korea (35-40°N, 124-131°E) and the rigidity modulus (μ) is assumed to be the standard value 3×10^{10} N/m² (Hanks and Kanamori, 1979), and thus the average seismic moment tensor and strain rates can be

Table 4. Principal strain rates derived from GPS velocity and Seismic data

	$\dot{\epsilon}_1$	$\dot{\epsilon}_2$	Azimuth
GPS	$(7.19 \pm 0.20) \times 10^{-9}$	$(-3.62 \pm 0.18) \times 10^{-9}$	-16.0
Seismicity	0.07×10^{-10}	-0.07×10^{-10}	-13.3

**Fig. 3.** The principal horizontal axes of the strain rate tensors in South Korea. The red arrows (thick lines) are GPS-derived strain rate and the blue arrows (thin lines) are seismicity-derived strain rate. The convergent arrows are contraction and the divergent arrows are extension.

obtained in this study region using the earthquake data during the time of 1936-2004 (Table 3). The principal seismicity strain rate is further obtained (Table 4). Figure 3 shows the principal seismic strain axis and the comparison between seismic and GPS strain rates. We note a good consistency between the two estimates (GPS and seismicity) of principal strain rate orientation, but the GPS strain rate is two orders of magnitude higher than seismicity one. This is due to using available and limited historic earthquake data in recently recorded events. In fact, the amplitude of the seismic strain rate strongly depends on the number of events in the historic earthquake catalogue.

4. CONCLUSION AND DISCUSSION

In order to further test the method to compute the strain rates with earthquake data, we compare the seismicity-derived strain pattern with source mechanism solutions of earthquakes. Figure 2 lists the epicentral distribution and

fault plane solutions (lower-hemisphere equal-area projection) for major events with $M_w > 4.0$ in and around the southern part of the Korean peninsula from 1936 - 2004. Solid and open quadrants denote the extension and compression, respectively. It can be seen that the extension and compression are NNW-SSE and ENE-WSW direction, respectively, consisting with seismicity-derived strain pattern. Furthermore, the seismicity-derived strain with the formulation of Kostrov (1974) has been confirmed by many recent cases, such as microseismic studies in the Zagros and Alborz (Hatzfeld et al. 2003) and studies of focal mechanisms from teleseismic waves (Talebian and Jackson, 2004). However, the seismic strain rate may be overestimated or underestimated depending the occurrence of earthquakes during the studied interval relative to the average recurrence interval of large earthquakes. In South Korea, on one hand, we cannot collect all historic earthquake catalogues due to many factors (e.g. war, disaster, etc.); on the other hand, the distribution of earthquakes in the time is not uniform. For example there were no large earthquakes between 1936 and 1963. Therefore, it is understandable that the seismic strain rate is lower than the GPS strain rate.

The crustal deformation in South Korea is analyzed based on three years of continuous GPS observations (2000-2003) and recently recorded seismicity data with $M_w > 4.0$ (1936-2004). The residual velocities of all GPS sites are small (average 1.5 mm/yr) with respect to the stable South Korea block, which suggests that the Euler vector can well represent the rigid block motion model of South Korea. Both geodetic and seismic strain rate tensors show that South Korea is dominated by both ENE-WSW compression and NWN-SES extension. The axes of the seismic strain rate tensor have consistent orientation and style with those deduced from the GPS velocity field in South Korea, indicating that a combined analysis of the strain rate field derived from GPS and seismicity allows us to accurately define the deformation style and pattern in South Korea. In addition, the consistent principal horizontal axes of both strain rate tensors reflect that the occurrence of shallow earthquakes in South Korea is closely related with the horizontal strain.

ACKNOWLEDGEMENTS. All figures were made with the public domain software GMT (Wessel and Smith, 1998). We are grateful to the National Geographic Information Institute (NGII), and the Ministry of Government Administration and Home Affairs (MOGAHA) and other members who made the GPS observation data available. This work was supported by the Korean Ministry of Science and Technology under grants M2-0306-01-0004, M6-0404-00-0018 and M6-0404-00-0010.

REFERENCES

- Aki, K., and Richards, P.G. 1980, Quantitative seismology: Theory and Methods, vol. 1 & 2. W.H. Freeman & Co., San Francisco,

- USA.
- Altamimi, Z., Sillard, P. and Boucher, C., 2002, ITRF2000: A New Release of the International Terrestrial Reference Frame for Earth Science Applications. *Journal of Geophysical Research*, 107(B10), 2214, doi: 10.1029/2001JB000561.
- Calais, E., Galisson, L., Ste'phan, J.F., Delteil a, J., Deverche' re a, J., Larroque, C., Mercier de Le'pinay, B., Popoff, M., Sosson, M., 2000, Crustal strain in the Southern Alps, France, 1948-1998. *Tectonophysics*, 319, 1-17.
- DeMets, C., Argus D. F., Gordon, R. G. et al, 1990, Current plate motions. *Geophysical Journal International*, 101, 425-478.
- Ekstrom, G. and Dziewonski, A.M., 1988, Evidence of bias in estimations of earthquake size, *Nature*, 332, 319-323.
- Hanks, T.C. and Kanamori, H., 1979, A moment-magnitude scale, *Journal of Geophysical Research*, 84, 2348-2350.
- Hatzfeld, D., Tatar, M., Priestley, K. and Ghafory-Ashitany, M., 2003, Seismological constraints on the crustal structure beneath the Zgros mountain belt (Iran), *Geophys.J.Int.* 155, 403-410.
- Jin, S.G. and Zhu, W.Y., 2004, A revision of the parameters of the NNR-NUVEL1A plate velocity model. *Journal of Geodynamics*, 38, 85-92.
- Jost, M.L. and Herrmann, R.B., 1989, A student's guide to and review of moment tensors. *Seismol. Rel. Lett.* 60, 37-57.
- Jun, M.S., 1993, Source properties of earthquakes in and around the Korean Peninsula. *Proceeding of Seismology in East Asia*, p. 170-173.
- Kato, T., Kaotake, Y., and Nakao, S., 1998, Initial results from WING, the continuous GPS network in the western Pacific area. *Geophysical Research Letters*, 125, 369-372.
- Kim, S.G. and Lee, K. S., 2000, Seismic risk map of Korea obtained by using South and North Korea Earthquake catalogues. *Journal of Earthquake Engineering Society of Korea*, 4, 1, 13-34.
- Kim, S.G., Lkhasuren, E. and Park, P.H., 2004, The low seismic activity of the Korean Peninsula surrounded by high earthquake countries. *Journal of Seismology*, 8, 91-103.
- Kogan, M.G., Steblov, G. M., King, R.W., Herring, T. A., Frolov, D. L., Egorov, S. G., Levin, V. Y., and Jones, A., 2000, Geodetic constrains on the rigidity and relative motion of Eurasian and North American. *Geophysical Research Letters*, 27, 2041-2044.
- Kostrov, B., 1974, Seismic moment and energy of earthquakes and seismic flow of rock. *Izvestia, Academic Sciences, USSR, Physics of the Solid Earth*, 1, 23-40.
- King, R.W. and Bock, Y., 1999, Documentation for the GAMIT GPS Analysis Software, Massachusetts Institute of Technology, Cambridge Mass.
- Masson, F., Chery, J., Hatzfeld, D., et al. 2005, Seismic versus aseismic deformation in Iran inferred from earthquakes and geodetic data. *Geophysical Journal International*, 160, 217-226.
- Molnar, P. and Tapponnier, P., 1975, Cenozoic tectonic of Asia: effects of a continental collision. *Science*, 189, 419-426.
- Wessel, P., and Smith, W. H. F., 1998, New improved version of Generic Mapping Tools released: Eos, *Transactions of American Geophysical Union*, 79, 579 p.
- Talebian, M. and Jackson, J.A., 2004, A reappraisal of earthquake focal mechanisms and active shortening in the Zagros mountain of Iran, *Geophys.J.Int.* 156, 506-526.

Manuscript received June 27, 2005

Manuscript accepted December 6, 2006